Hindawi
Journal of Chemistry
Volume 2022, Article ID 8759235, 11 pages
https://doi.org/10.1155/2022/8759235

Research Article

An Industrial Approach to Production of Tofacitinib Citrate (TFC) as an Anti-COVID-19 Agent: A Joint Experimental and Theoretical Study

Seyyed Amir Siadati,[1] **Mehdi Soheilizad**,[1] **Loghman Firoozpour**,[1,2] **Marjan Samadi**,[1] **Meghdad Payab**,[3] **Saeed Bagherpour**,[1] **and Seyyed Mehdi Mousavi**[1]

[1]*Department of Research & Development, Parsian Pharmaceutical Technology Company, Alborz, Tehran, Iran*
[2]*Department of Medicinal Chemistry, Faculty of Pharmacy, The Institute of Pharmaceutical Sciences (TIPS), Tehran University of Medical Sciences, Tehran, Iran*
[3]*Faculty of Chemistry, University of Mazandaran Babolsar, P.O. Box 47416-95447, Babolsar, Mazandaran, Iran*

Correspondence should be addressed to Seyyed Amir Siadati; chemistry_2021@yahoo.com

Received 30 November 2021; Revised 7 September 2022; Accepted 7 November 2022; Published 9 December 2022

Academic Editor: Ashanul Haque

In this report, we have presented our experience about a facile method for synthesis of tofacitinib citrate (TFC). The developed analytical methods for identification and qualifications are also included. As TFC seems to be effective in treatment of the symptoms of COVID-19 (SARS family), manufacturing of this active pharmaceutical ingredient (API) could be helpful. The API of TFC was prepared from the diamine intermediate in an ambient and solvent-free condition. Elimination of the reaction solvent resulted in decreasing the cost and preventing the rejection of the organic volatile impurity (OVI) test. The final citrate addition step was carried out using water as a solvent (the citrate content was 37.5% by potentiometry). Moreover, the results of the Karl-Fischer (KF) titration analysis was about 0.24%, which showed that the use of water does not increase the water content of the crystal structure.

1. Introduction

In late 2019, the outbreak of a newly mutated version of the SARS family (named COVID-19) was first reported in Wuhan, China [1]. Among the victims of that virus were the medical staff and other groups who dedicated their lives to saving people [2]. In parallel with clinical therapies, scientists began to review the reports [3, 4], in order to investigate the behavior of the virus. Such understanding led researchers to find probable ways, which would help control this infecting virus [5–7]. Then, attempts to make vaccines [8], synthesis of effective drugs [9, 10], and even use of special diets as well as traditional medicine [11, 12] were started. Since experts truly predicted that finding a safe vaccine and beginning the mass vaccination process might take a long time (at least about several months), efforts to find effective chemical or biochemical drugs were started [13]. For example, reports for the successful use of umifenovir, favipiravir, and remdesivir (Figure 1) attracted the attention of scientists. Somehow, many experts started to find new or more facile ways for synthesizing these drugs [14]. Easier, cheaper, or greener ways for synthesizing selected organic compounds have always been important for the involved researchers [15–17].

Tofacitinib compound in the citrate form has recently reported to be effective in treatment of the symptoms of COVID-19 [18, 19]. Thus, developing the synthesis procedure and scaling up of this API may be beneficiary. Therefore, in the present report, we have shared our results about an easy approach for solvent-free N-acylation of the tofacitinib freebase (and the subsequent citrate addition in water as solvent in one pot) (Scheme 1). To give a

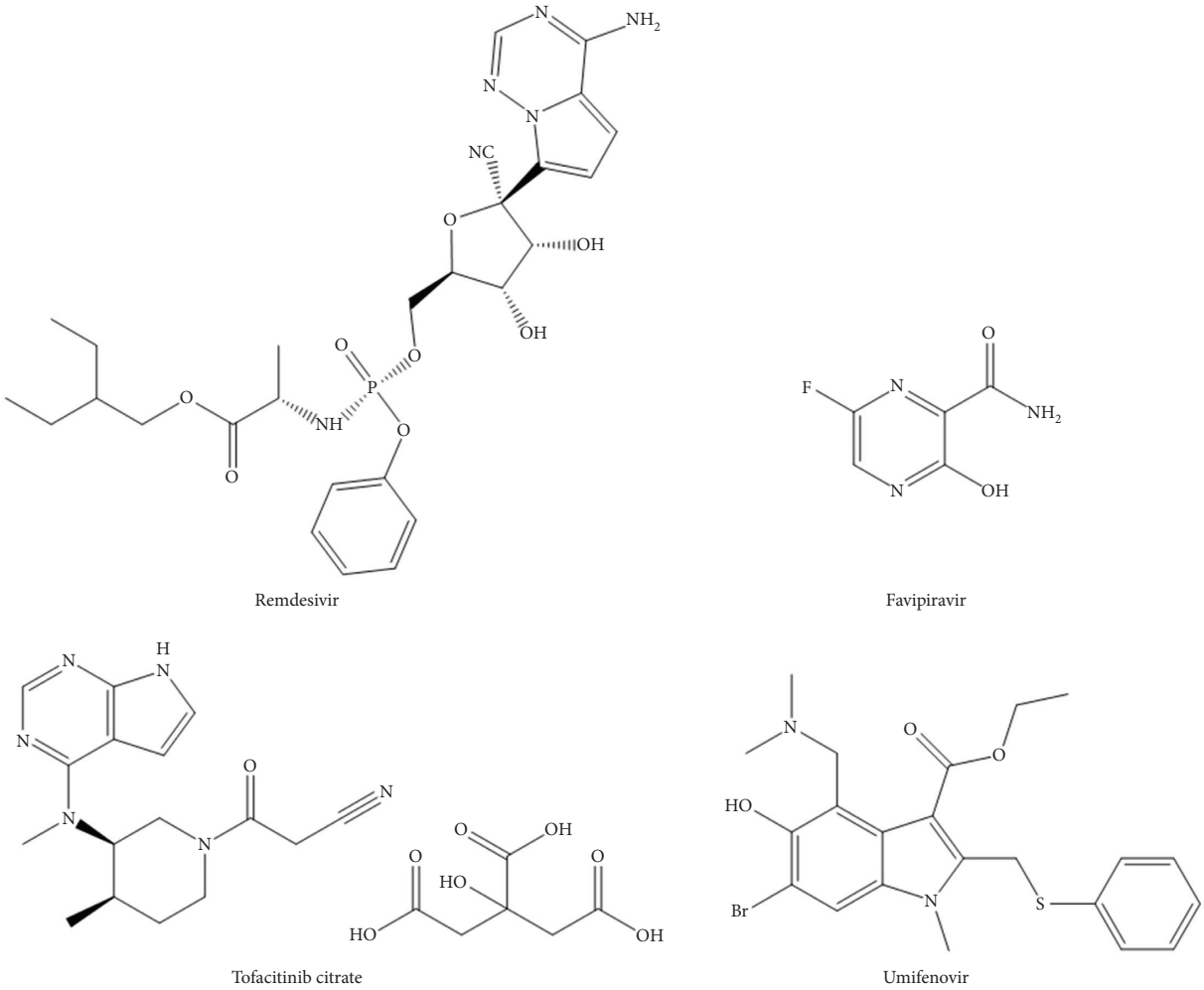

Figure 1: Chemical structures representing remdesivir, favipiravir, umifenovir, and tofacitinib citrate.

comprehensive insight, the results of the previous studies (in terms of yield, solvent, catalyst, and other reaction conditions) are also compared with the outcome of this project (Table1). Maricán et al., for example, have used dichloromethane (DCM) as a solvent using 3-(ethyliminomethyleneamino)-N,N-dimethyl-propan-1-amine/N-hydroxybenzotriazole (EDC/HOBT) as an activating agent at room temperature to give tofacitinib citrate (TFC) in an 80% yield [20]. Zhi et al. have applied 1,8-diazabicyclo[5.4.0] undec-7-ene (DBU) as a mild organic base to n-butanol as a solvent at 100°C for 24 hours, resulting in an 87% crude product [22]. Ruggeri et al. reported the trimethylamine (TEA) base in DCM (67.3%) and toluene (65.3%) as solvents at −5°C and 100°C, respectively [21]. Five years later in 2017, Bonanomi et al. have used DBU in n-butanol as a solvent at 40°C for 18 hours, which gave an 87.6% product [23]. Patil et al. reported the reaction in the same condition at 45°C without stating the reaction time [24]. Also, Cai et al. previously introduced a DBU/butanol system for 20 hours, resulting in 93% yield [25]. Rajan et al. used ethanol instead of n-butanol in the presence of DBU, which led to a considerable decrease in the yield [26]. Xu et al. and Xiao et al. have used HOBT/DCM and DBU/ACN, respectively. It resulted in about 70% yield [27, 28]. However, the DBU/ACN system has demonstrated a shorter reaction time (6 hours compared to 12 hours for the HOBT/DCM system).

2. Materials and Methods

2.1. Reagents and Instrumentation. All chemical reagents and solvents were obtained from commercial sources and used without further purifications. All of the analytical thin layer chromatography (TLC) tests were performed on silica gel 60 F254 precoated plates. The melting point was corrected. The infrared spectra (IR) were recorded as thin films on potassium bromide (KBr) plates with îmax in inverse centimeters. The hydrogen nuclear magnetic resonance (1H-NMR) spectrum was taken in commercial deuterated solvents using a multinuclear spectrometer (Varian, INOVA400 MHz). All of the chemical displacements (of 1H NMR) were reported in parts per million (ppm) relative to internal tetramethylsilane (TMS, ppm 0.0) or with the solvent reference relative to TMS which was employed as an internal standard (DMSO-D6, 2.500 ppm). Data were reported as follows: chemical shift (multiplicity (singlet (s), doublet (d), triplet (t), quartet (q), broad (br), and multiplet

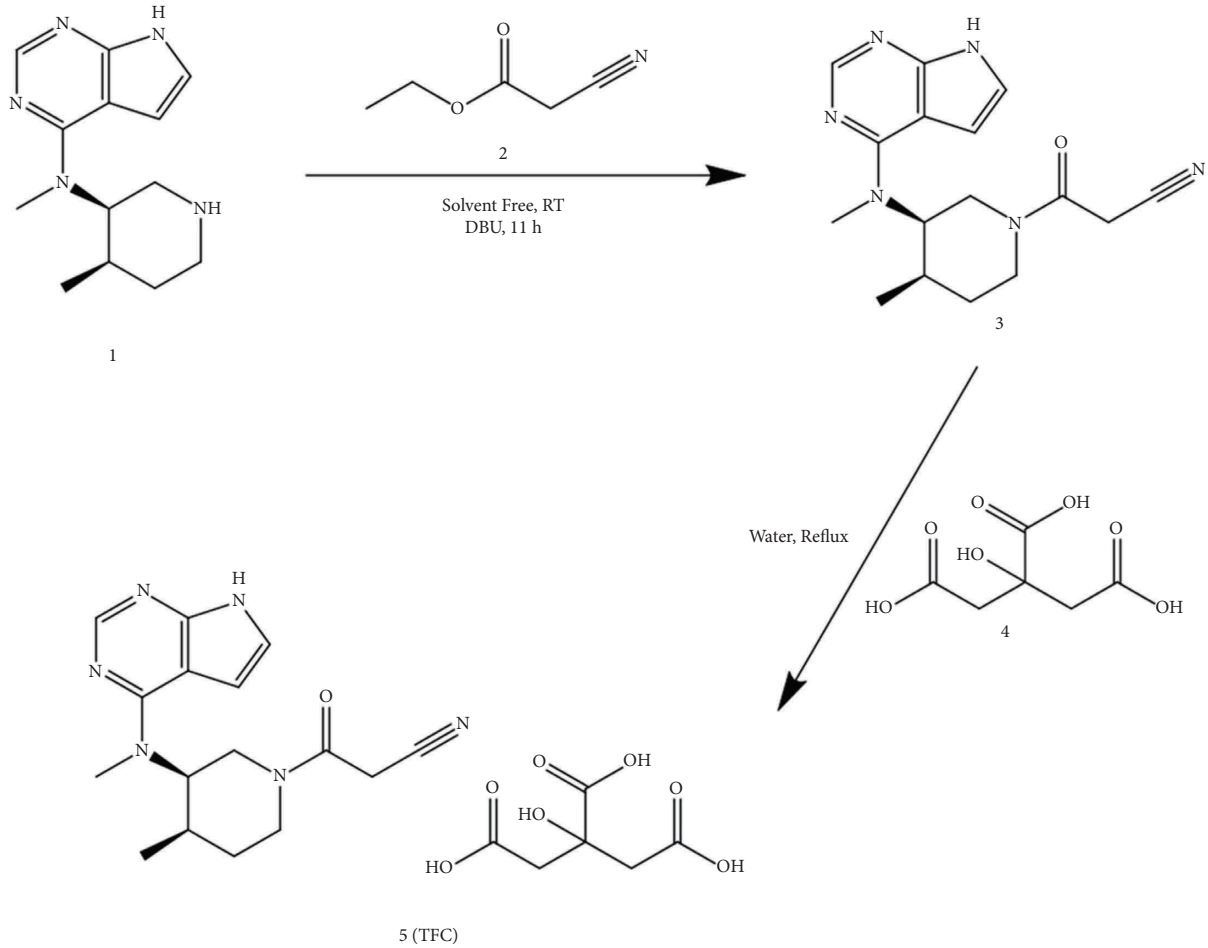

Scheme 1: One-pot N-acylation and subsequent citrate addition of intermediate **1** to yield TFC.

(m)), coupling constants (Hz), and integration). The 13 C NMR spectrum was taken by using a multinuclear spectrometer (100 MHz) and diluted solutions of the resulting compound in DMSO-d6 as the solvent. Also, chemical shifts were reported in ppm (ppm unit) downfield from tetramethylsilane as an internal standard (CDCl3, ppm 77.0). The mass spectra were obtained utilizing electron impact (EI) at an ionizing potential of 70 eV. The OVI test was carried out using a gas chromatography-flame ionization detector (GC-FID) system (CP-3800, GC Varian, equipped with CTC Combi-Pal headspace autosampler injection containing an incubator). A capillary column (Agilent J&W CP-Select 624 CB, length 30 m, internal diameter 0.53 μm, and film thickness 3.0 μm GC column, with an optimized G43 stationary phase) was used for the separation of gaseous species. The carrier gas was nitrogen, and the flow rate was 6 ml·min^{-1}. The potentiometric titration analysis for calculating the citrate content in TFC was performed by using a computer-controlled titration system made by Metrohm (Filderstadt, Germany), with corresponding commercial software (PC control). The setup consisted of a titration instrument (Titrando 805, Metrohm). 200 mg of the sample was dissolved in 50 ml of acetic acid and then titrated by 0.1 N perchloric acid solution.

An Agilent 1260 high-performance liquid chromatography (HPLC) system (Agilent Technology), equipped with a G1311BLC pump, a G1316A column oven, and a G4212B UV-Visible detector, was used for all of the HPLC analyses. Also, a C18, end-capped (25 × 4.6) mm, 5 μm liquid chromatography column was used for the related substance analysis of TFC. Mobile phase A could be dibasic potassium phosphate buffer at pH 3.5, mobile phase B could be 100% acetonitrile (ACN), and the diluent is methanol (MeOH). The flow rate of the eluent was 1.0 ml·min^{-1}. The column oven temperature was 30°C, and the spectrum was recorded at 290 nm. Table 2 shows the gradient of elution.

2.2. Synthesis and Characterization

2.2.1. Representative Procedure for the Synthesis of TFC via Solvent-Free Reaction. About500 g (2.04 mol) of intermediate **1** is dissolved in 342 ml (2.86 mol) of ethyl cyanoacetate **2**. Then, 475 ml (3.06 mol) of 1,8-diazabicyclo[5.4.0]undec-7-ene (DBU) is added to the mixture dropwise. For better mixing, 20 ml of MeOH is added to the mixture. The reaction is stirred for about 11 hours. By monitoring the reaction progress by the thin-layer chromatography (TLC) method, it could be observed that the reaction is completed in 11 hours. After

Table 1: A comparison between the examples of the previous reports and the present work.

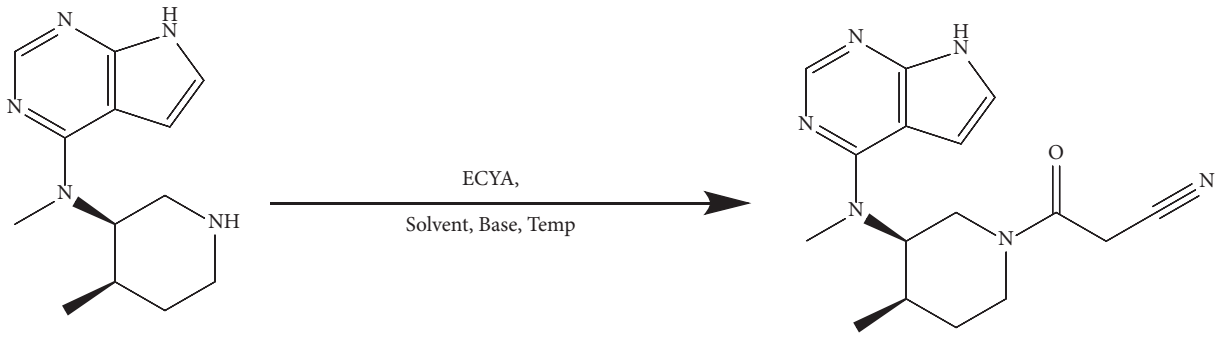

1 3

Entry	Catalyst	Solvent	Temperature (°C)	Time (h)	Yield (%)	Type of workup	Ref
1	EDC/HOBT	DCM	R.T	12	80	Precipitation	[20]
2	TEA	Toluene	100	24	65.3	Extraction	[21]
3	TEA	DCM	−5	3.5	67.3	Extraction	[21]
4	DBU	n-butanol	40	18	87.6	Precipitation	[22, 23]
5	DBU	n-butanol	45	Not stated	85	Precipitation	[24]
6	DBU	n-butanol	40	20	93	Precipitation	[25]
7	DBU	Ethanol	R.T	6	50	Precipitation	[26]
8	HOBT	DCM	R.T	12	70	Extraction	[27]
9	DBU	ACN	40	6	72	Precipitation	[28]
10	DBU	—	R.T	11	95.1	Precipitation	This work

Table 2: The proposed gradient for the elution of the HPLC analysis of the API of TFC.

Time	Flow rate (ml·min^{-1})	Phase A %	Phase B %
0	1.0	75	25
5	1.0	75	25
20	1.0	30	70
45	1.0	30	70

completing the N-acylation reaction that gives tofacitinib in the freebase form, 780 g (4.1 mol) of citric acid (which was previously dissolved in 500 ml of water) is added to the reaction mixture. Then, the temperature is increased up to 80°C. The mixing process at 80°C is continued for about 50 minutes, and then, the temperature is decreased to 25°C while stirring for about 5 hours. The resulting precipitate is filtered and washed with 500 ml of water 3 times. The crude product is recrystallized in a MeOH-water mixture under reflux conditions (yield = 959 g; 93.1%). The eluent (mobile phase) of the TLC method is (toluene : acetone : ethanol : TEA) with a ratio of (45 : 45 : 7 : 3). Also, the retention factor (Rf) values are 0.3 and 0.73 for intermediate **1** and ECYA-DBU complex **2** (relative to the STD of TFC), respectively. The melting point of the product is about 217°C. The infrared spectra on KBr plates are as follows: 3119, 2955, 1720, 1618, 1600, 1535, 1450, 1409, 1373, 1348, 1225, 1183, 1052, 904, and 732 cm^{-1} [20]. The proton NMR spectra of product ^{1}H-NMR (400 MHz, DMSO-d6) δ are as follows: 0.97–0.99 (d, 3H), 1.51–1.86 (m, 2H), 2.33–2.46 (m, 1H), 2.65–2.80 (ABq, J = 15.2 Hz, 4H), 3.18–3.26 (m, 3H), 3.37–3.45 (m, 1H), 3.6–4.15 (m, 4H), 4.85 (s, 1H), 6.56 (s, 1H), 7.15 (d, J = 2.8 Hz, 1H), 8.13 (d, J = 5.6 Hz, 1H), and 11.63 (s, 1H) and ^{13}C NMR (100 MHz, DMSO-d6): 175.2, 171.8, 161.8,157.2, 151.8, 150.7121.3,116.6, 105.6, 102.3, 72.9, 53.3, 43.3, 42.2, 34.5, 31.4, 30.5, 25.4, and 14.1. The data for the CHN elemental analysis are C, 52.40; H, 5.60; N, 16.65; and O, 25.38 (experimental) and C, 52.38; H, 5.59; N, 16.66; and O, 25.37 (calculated by ChemDraw). Also, the mass spectrum MS (m/z) of the product is 313.17 (M^{+1}) [22].

2.2.2. Representative Procedure for the Synthesis of TFC via the DMF-K_2CO_3 System. About 10 g (41 mmol) of intermediate **1** is dissolved in 100 ml DMF. About 8 g (75 mmol) of ECYA **2** is added to the mixture. Then, 2 g of K_2CO_3 (0.015 mmol) is added to the reaction mixture. The reaction is heated at 50°C for about 11 hours. By monitoring the reaction progress by the TLC method, it is observed that the reaction is completed in 11 hours. After completing the N-acylation reaction that gives tofacitinib in the freebase form, 23 g of citric acid salt (which was previously dissolved in 30 ml of water) is added to the reaction mixture, and the temperature is increased up to 80°C. The mixing process at 80°C is continued for about 50 minutes, and then, the temperature is decreased to 0°C while stirring for about 5 hours. The resulting precipitate is filtered

and washed with 10 ml of water 3 times. The crude product is recrystallized in a MeOH-water mixture under reflux conditions (yield = 37.0%).

2.2.3. Representative Procedure for the Synthesis of TFC via the Ethyl Acetate-Triethylamine (EtOAC-TEA) System. About 10 g (41 mmol) of intermediate **1** is dissolved in 100 ml EtOAC. About 8 g (75 mmol) of ethyl cyanoacetate **2** is added to the mixture. Then, 12 ml of TEA (120 mmol) is introduced to the reaction vessel. The reaction is left at 50°C for about 11 hours. By monitoring the reaction progress by the TLC method, it is observed that the reaction is completed in 11 hours. After completing the N-acylation reaction that gives tofacitinib in the free-base form, the EtOAC solution was concentrated by using a rotary evaporator to give a yellow oily matter (yield = 45.0%).

2.3. Theoretical. Several hypothetical structures with different orientations were developed as input files for tofacitinib (freebase) and the TFC API, both in the gas phase. The input files were then processed by using the Gaussian 03 quantum chemical package [29] at a B3LYP/6-311G(d, p) level of theory to give possible stable and metastable states. Among all detected species, the most stable state was selected for further investigations. Geometrical structures, frontier molecular orbitals (FMOs), and the theoretical UV-visible spectrum were calculated (all in the gas phase) and presented in the manuscript accordingly. The previous reports showed the suitability of the mentioned basis set for such calculations [30]. Also, the key parameters for reactivity descriptors are calculated by the following formula [31–34].

Global hardness is expressed as follows:

$$\eta = \frac{(I - A)}{2(1)}. \tag{1}$$

Softness is expressed as follows:

$$\eta = \frac{1}{2\eta}. \tag{2}$$

Electronegativity is expressed as follows:

$$\chi = \frac{(I + A)}{2}. \tag{3}$$

The electrophilicity index is expressed as follows:

$$\omega = \frac{\mu^2}{2\eta}, \tag{4}$$

where I is the ionization potential which is the negative of the energy level of HOMO ($-E_{HOMO}$), A is electron affinity which is the negative of the energy level of LUMO ($-E_{LUMO}$), and μ is the chemical potential.

$$\mu = \frac{(I + A)}{2}. \tag{5}$$

3. Results and Discussion

3.1. Synthesis. As given in Table 1, there are a few reports revealing exact procedures for tofacitinib citrate (TFC) synthesis *via* its N-acylation process [20–28]. A glance at the data presented in the aforementioned table shows that all N-acylation processes by using ethyl cyanoacetate need base catalyzing agents. The type of solvent used for the reaction determines the type of the applied base. In entries 1, 3, and 8 (Table 1), dichloromethane (DCM) was applied as a solvent. Due to low boiling point of DCM, the reaction temperature is usually lower than about 35°C. The reports show that in this solvent, the catalyst is usually hydroxybenzotriazole (HOBT), or trimethylamine (TEA). The advantage of using DCM as a solvent is its hydrophobic nature, which helps the reaction progress. However, it would lead to emergence of a variety of impurities. On the other hand, it should be noted that the use of DCM requires the costly and time-consuming extraction process.

Choosing alcohols as solvents (entries 4–7, Table 1) usually require organic bases such as TEA, diethylamine (DEA), and 1,8-diazabicyclo[5.4.0]undec-7-ene (DBU). The use of DBU (in comparison to TEA) has the advantage of higher boiling point, which allows for setting higher temperatures, facilitating the reaction in terms of lower completion time. Anyway, some researchers reported different yields for DBU-alcoholic systems (from 50% to 87.6%). Also, a report (entry 9, Table 1) revealed the use of ACN as a solvent with DBU as a catalyst, which resulted in a 72% yield.

In this work (Table 3), we have used some solvents containing DMF, MeOH, EtOAC, and water. Finally, we have examined the solvent-free condition. Moreover, three different bases (TEA, DBU, and K_2CO_3, as organic and inorganic bases, respectively) were applied. Our observations showed that using water as a solvent would not give satisfying results. This might be caused by the low miscibility of water and the ethyl cyanoacetate (ECYA)-intermediate system. Use of DMF as a solvent (with K_2CO_3 or TEA) could accelerate reaction progress. However, it results in a dirty impurity profile (entries 1 and 2 in Table 3). In these cases, the crude product of these systems must be purified by using a chromatography column. Also, choosing EtOAC as a solvent may be beneficial in view of the hydrophobic nature. It is expected that this reaction gives the highest yield, while the experimental results were not considerably good (entries 3 and 4, Table 3). The isopropanol-mediated system (entries 5 and 6, Table 3) representing alcoholic mediums gives a relatively good yield, but like some other reports, the reaction time is long and its impurity profile is not clean.

These observations, as well as some other benefits such as low cost, easy workup, probable higher rates, and resolving OVI problems, lead to design of a scheme in which intermediate **1** is reacted with ECYA in a solvent-free condition. However, in spite of the liquid nature of ECYA, compound **1** could not be dissolved in ECYA. On the other hand, the instruction of some previous reports containing the addition of ECYA-DBU mixture to the intermediate leads to a hard creamy precipitate. Thus, after some tests, we have found out the true order of addition. First, intermediate **1** is added to a

Table 3: Optimization of the N-acylation reaction conditions in view of solvents, bases, and temperature.

Entry	Catalyst	Solvent	Temperature (°C)	Time (h)	Yield (%)	Type of workup
1	K_2CO_3	DMF	50	11	37.0	Precipitation
2	TEA	DMF	50	11	50.2	Precipitation
3	TEA	EtOAC	R.T	11	45.0	Extraction
4	DBU	EtOAC	R.T	11	67.3	Extraction
5	DBU	Isopropanol	55	17	73.5	Precipitation
6	TEA	Isopropanol	55	17	45.0	Precipitation
7	TEA	Water	50	24	—	—
8	DBU	Water	50	24	—	—
9	K_2CO_3	Water	50	24	—	—
10	DBU	—	−10	11	—	—
11	DBU	—	0	11	—	—
12	DBU	—	R.T	11	93.1	Precipitation
13	DBU	—	50	11	95.6	Precipitation

vessel containing ECYA. Then, DBU is dropped to the vessel while stirring. For better mixing, only a little portion of MeOH is added to the mixture (about 10% of the net weight of the intermediate). In such a system, the reaction rate is faster than that in previously reported conditions due to the increase in the concentration of the two intermediates.

Also, this solvent-free system handles to run the citrate addition process by a one-pot procedure (in water as solvent). The use of water as the reaction solvent following a solvent-free step makes the OVI test easier to pass. Thus, after completion of the N-acylation reaction, a certain amount of citric acid along with a portion of water is added to the reaction vessel (according to the description of the previous section). Also, at temperatures below room temperature (about 25°C), the reaction mixture would be creamy and the magnet (or paddle) could not move around, while at temperatures up to 50°C, the reaction mixture would be more fluid and the yield might increase. Finally, our experiments showed that this acylation reaction is not possible without a catalyst, at least in all entries of Table 3.

3.2. Pharmaceutical Analytics. First, the HPLC instrument was used for pharmaceutical analytical identification (*via* comparison with the retention time (RT) of the TFC standard) and for assaying the drug content in the synthesized sample, where mobile phase A is dibasic potassium phosphate buffer at pH 3.5, mobile phase B is 100% ACN, and the diluent is MeOH. The flow rate is 1.0 ml·min^{-1}, the column oven temperature is 30°C, and the spectrum is recorded at 290 nm.

As shown in Figure 2, the purity of the purified sample is about 99.73%, and the amount of each impurity is about 0.05%. It shows that the API is suitable in view of the related impurity profile.

Next, the water content has been determined by using the KF titration method. This analysis gives some important information about the residual water in API. There should not be crystal-trapped water molecules in pharmaceutically suitable polymorph of TFC. Also, the total water of API must be lower than 1% according to guidelines [32]. The percentage of the KF of the crude sample is about 0.24% which is satisfying due to the standards. Moreover, the results of the OVI analysis showed that there is not any out of limit solvent residue in the API powder. It is thought that the use of water as the solvent in the last step of synthesis might eliminate unpleasant solvent residues.

Finally, potentiometric titration could determine the citrate content of the API of TFC. This analysis should be performed for investigating the suitability of the citrate addition process. To do so, 100 mg of the TFC sample is dissolved in glacial acetic acid and is titrated with 0.1 N perchloric acid (Figure 3). The result shows that the citrate content of the sample (37.5%) is in the acceptable range (36.2%~40%).

3.3. Theoretical Results. As mentioned above, at the first step, the geometrical structure of TFC molecules has been developed as the Gaussian input file in different orientations in the gas phase to find the most stable state. Then, the calculation method and the basis set are updated at the B3LYP/6-311G(d,p) level of theory in the output file. To investigate the accuracy of our theoretical calculations, the experimental UV-visible spectrum (λ_{max} = 287 nm) [35] is compared with theoretical time-dependent density functional theory (TD-DFT) [36] (λ_{max} = 280 nm–285 nm). Figure 4 shows the UV-visible spectrum obtained by the TD-DFT method.

After extraction of the UV-visible spectrum from the optimized geometrical structure of TFC and comparing it with the experimental result, the FMO of the system as well as geometrical parameters were investigated. Figure 5 represents the results of the FMO analysisof the TFC molecule. moreover, this figure shows the optimized structure of this molecule both in side, and in upper view. As shown in the figure, the HOMO orbital has mainly been located on tofacitinib parts (especially on cyano and aromatic rings). It would show the importance of those groups in interaction with receptor parts.

Also, the geometrical structure of TFC indicates that this system would be more stable when tofacitinib changes into a sandwich-like system to make maximum hydrogen bonds with citric acid (Figure 5, side view C). As shown in part (e), there are five major hydrogen bonds between tofacitinib and citrate fragments. In one side, O21-H41 (1.71 Å) and O39-H30 (2.24 Å) are formed, while on the other side, O46-H8

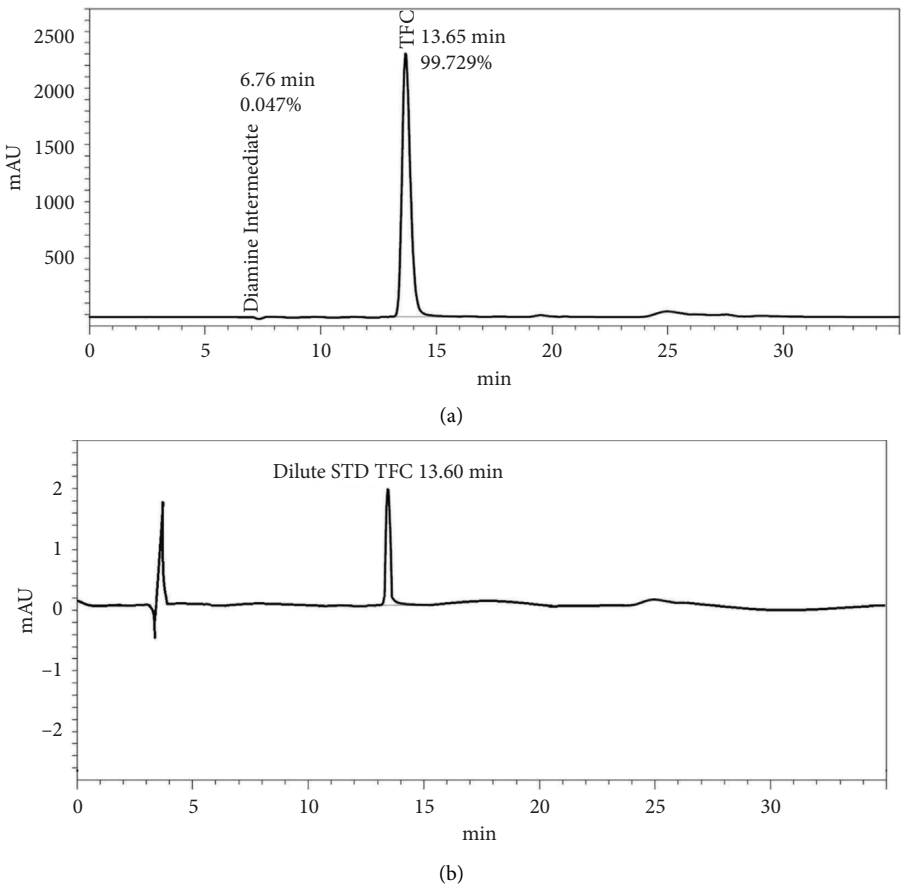

Figure 2: The chromatograms of the related impurity analysis for the TFC sample at 1000 ppm (a) and for the diluted standard at 1 ppm (b) concentration prepared by using the reverse phase HPLC system.

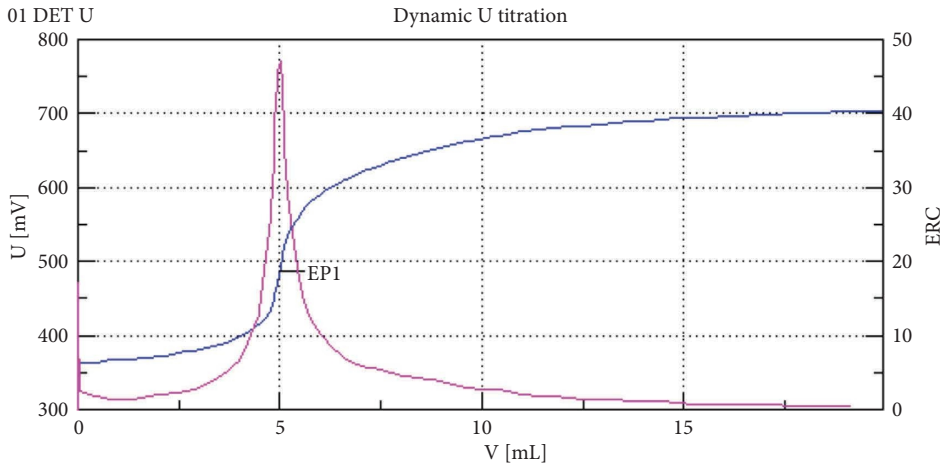

Figure 3: The chromatogram of the potentiometric titration for assaying the TFC content in the crude sample in perchloric acid.

(2.11 Å), O43-H8 (2.37 Å), and N12-H44 (1.90 Å) are detected. Also, there are several intermolecular hydrogen bonds. It seems that such tied interactions result in the decrease in potential energy and stabilization.

On the other hand, the DFT approach has been confirmed to be an efficient method to provide theoretical insights into chemical reactivity and substrate selectivity in terms of popular qualitative chemical concepts, such as the electrophilicity index (ω), electronegativity (χ), softness (S), chemical potential (μ), and chemical hardness (η). Also, with the aid of electron affinity (A), Koopmans' theorem ionization potential (I), hardness (η), softness (S), and electronegativity (χ), which are based on the energy of HOMO and LUMO, some of the physiochemical behaviors of the system could be predicted. The data presented in Table 4 indicate the reactivity parameters for TFC compounds. The

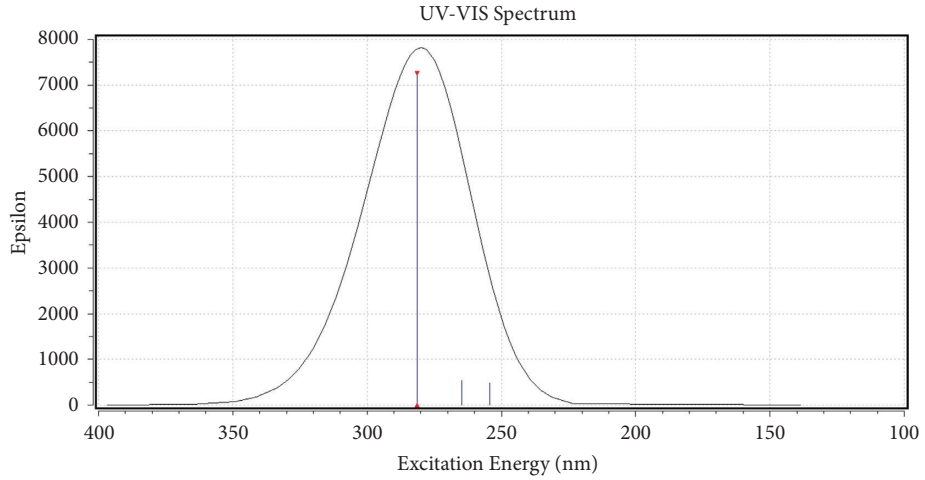

Figure 4: The UV-visible spectrum of TFC obtained by the DT-DFT method at the B3LYP/6-311G(d,p) level of theory.

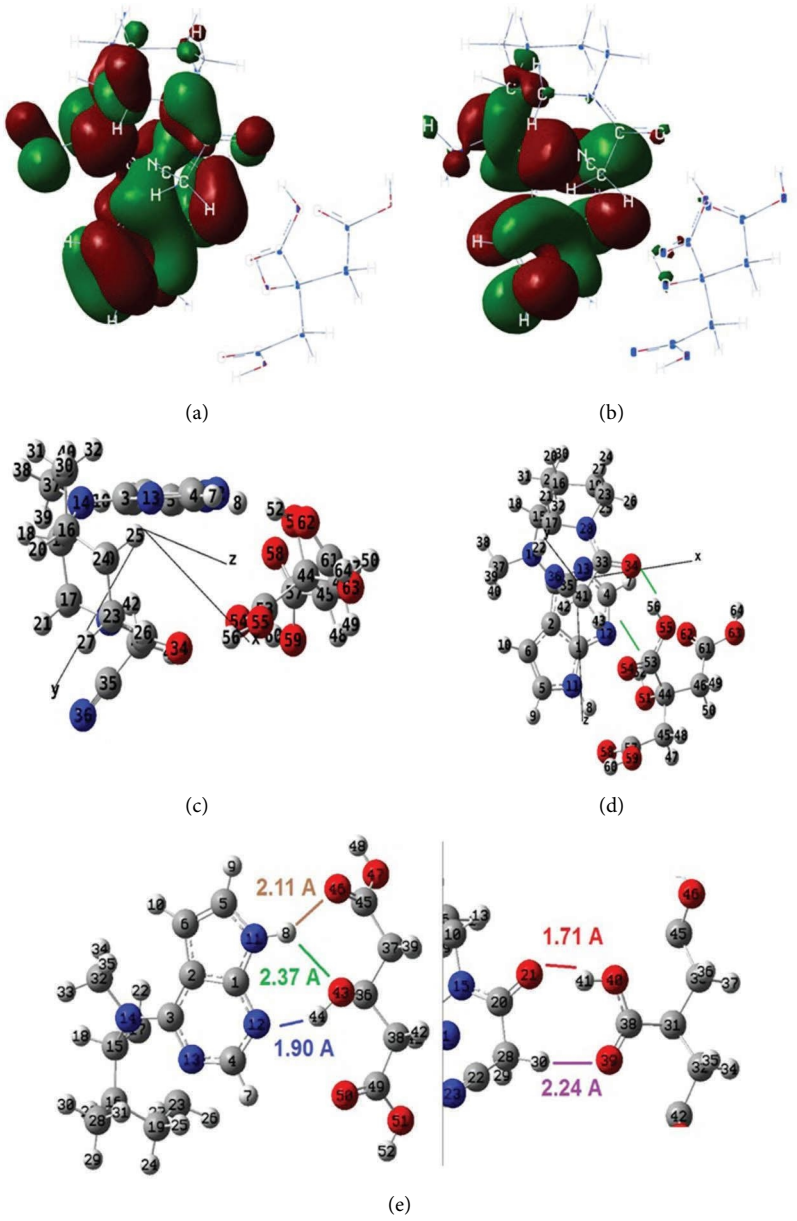

Figure 5: HOMO and LUMO (FMO) orbitals of TFC as well as the geometrical structure of the most stable state of TFC optimized at the B3LYP/6-311G(d,p) level of theory. (a) TFC HOMO. (b) TFC LUMO. (c) TFC (side view). (d) TFC (upper view). (e) TFC.

Table 4: The reactivity descriptors of tofacitinib citrate compounds.

Reactivity descriptor	Reactivity descriptor energy (a.u.)
Electron affinity	0.0354
Ionization potential	0.2129
Global hardness	0.0887
Softness	5.637
Electronegativity	0.1241
Electrophilicity index	0.0868
HOMO energy	−0.2126
LUMO energy	−0.0354

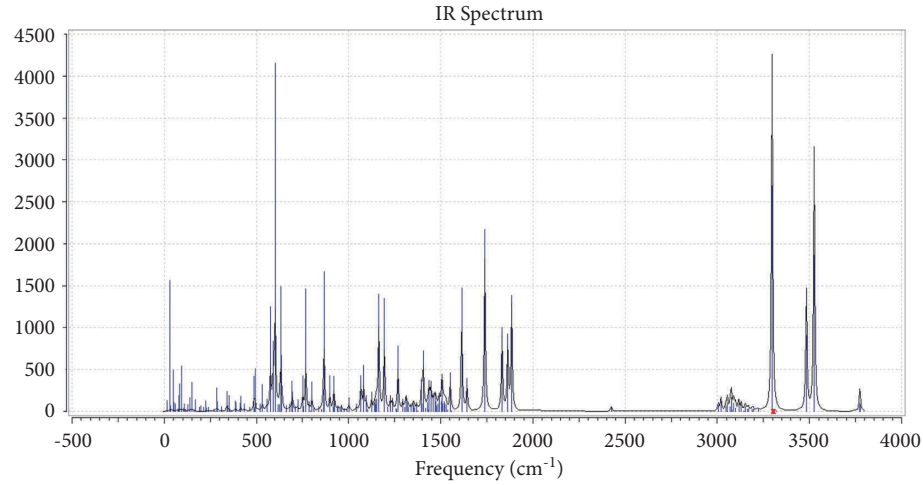

Figure 6: The calculated IR spectrum for TFC compounds.

results indicate that the HOMO-LUMO energy gap of TFC is about 0.1772 a.u., which is relatively low. Somehow, it could reveal its polarizable nature (due to its low FMO gap, low kinetic stability, and high chemical reactivity). Moreover, low ionization energy (I) about 0.2129 a.u. of TFC reveals that this compound is highly reactive. Also, the softness parameter has been used to measure the extent of chemical reactivity and is the measure of the capacity of an atom or group of atoms to gain electrons. Thus, softness (5.637 a.u.) of TFC indicates that it is a compound that could be soft enough to receive electron density from different types of compounds (Table 4). Here, it could be concluded that the softness of TFC might be a parameter for increasing its activity for inhibition of Janus kinase (Jak)-mediated signaling. Recent reports stated that smaller energy gaps could easily transit from HOMO to LUMO, which is important for the molecular reactivity of those matters. Since the decrease in the electronegativity index is proportional to the increase in inhibitive abilities [37], thus, the lower electronegativity of the TFC molecule leads to higher inhibitory effects on it. The statistical amounts of the calculated molecular descriptors are presented in Table 4. The smaller energy gap, lower electronegativity, and higher dipole moment that are crucial for the inhibitory effect of a molecule were observed, which validates better inhibitory effects for the selected compounds [37, 38]. Moreover, the results of previous reports have also confirmed that there is a good correlation with a single parameter, and hence, compelling evidence is provided that electrophilicity is a suitable descriptor of biological activity [39, 40].

Figure 6 represents the calculated IR spectrum of TFC. As shown in the spectrum, there are three main peaks at 3300–3600 cm^{-1}, which could be referred to O-H strength vibrations of citric acid, and a weak peak at 3040 cm^{-1}, which might be due to N-H strength vibration of pyrrole and C-H bonds of aromatic rings. However, in the experimental IR spectrum, only one wide and strong peak (3119 cm^{-1}) could be observed, which is due to hydrogen bonding in the presence of citric acid. Also, there are some weak peaks at 2980–3000 cm^{-1} in the calculated IR spectrum due to aliphatic C-H bonds, which could be seen in the experimental data as well. Moreover, there are about five major peaks between 1600 cm^{-1} and 1860 cm^{-1} in the theoretical spectrum, which are referred to C=O bonds of citric acid on the one hand, and C=N, and C=C bonds of aromatic rings of tofacitinib on the other hand. Three strong peaks are observed at 1720 cm^{-1}, 1618 cm^{-1}, and 1600 cm^{-1}, which could be seen in the experimental chromatogram, respectively. In addition, two major peaks at 1910 cm^{-1} and 1100 cm^{-1} in the theoretical spectrum represent C-N vibration frequencies, which might be equal with two peaks at 1052 cm^{-1} and 904 cm^{-1} in the experimental chromatogram, respectively. Finally, the major peak at 760 cm^{-1} in theoretical calculation might be equal with the significant peak at 732 cm^{-1} in the experimental FT-IR spectrum.

4. Conclusion

The results of the project have demonstrated that the solvent-free N-acylation of the amine-intermediate leading to the formation of Tofacitinib in a higher yield, is possible in an aerobic condition, at room temperature(about 93.1%). Moreover, the one-pot citrate addition of the tofacitinib freebase to give TFC was carried out in water as a solvent.

Beside the low cost and the safe operating procedure, the use of water as a solvent in the last step of synthesis of API could lead to a decrease in the amount of hazardous residues of solvents (in the crystal structure). The results of the OVI analysis obtained by GC-FID, confirmed our predictions. Moreover, the KF test of TFC (about 0.24%) showed that the use of water in the last step does not increase the total water content of the crystal structure. Finally, the comparison between calculated ($\lambda_{max} = 280\,nm–285\,nm$) and experimental ($\lambda_{max} = 287\,nm$) UV-visible λ_{max} confirmed our theoretical calculations.

Data Availability

The experimental ^{1}H NMR, ^{13}C NMR, and the GC-FID spectra as well as the optimized geometry of TFC compounds used to support the findings of this study are included within the supplementary information file(s).

Conflicts of Interest

The authors declare that they have no conflicts of interest.

Supplementary Materials

The experimental ^{1}H NMR, ^{13}C NMR, and the GC-FID spectra as well as the optimized geometry of TFC compound are embedded in the supplementary information file(s). (*Supplementary Materials*)

References

[1] F. Ndaïrou, I. Area, J. J. Nieto, and D. F. M. Torres, "Mathematical modeling of COVID-19 transmission dynamics with a case study of Wuhan," *Chaos, Solitons & Fractals*, vol. 31, Article ID 109846, 2020.

[2] X. Zhang, X. Wang, X. Jia et al., "Risk factors for disease severity, unimprovement, and mortality in COVID-19 patients in Wuhan, China," *Clinical microbiology and infection*, vol. 26, no. 6, pp. 767–772, 2020.

[3] K. Yuki, M. Fujiogi, and S. Koutsogiannaki, "COVID-19 pathophysiology: a review," *Clinical Immunology*, vol. 215, Article ID 108427, 2020.

[4] M. Ciotti, S. Angeletti, M. Minieri et al., "COVID-19 outbreak: an overview," *Chemotherapy*, vol. 64, no. 5-6, pp. 215–223, 2019.

[5] B. Shah, P. Modi, and S. R. Sagar, "In silico studies on therapeutic agents for COVID-19: drug repurposing approach," *Life Sciences*, vol. 252, Article ID 117652, 2020.

[6] Z. Reiner, M. Hatamipour, M. Banach et al., "Statins and the COVID-19 main protease: in silico evidence on direct interaction," *Archives of Medical Science*, vol. 16, no. 3, pp. 490–496, 2020.

[7] M. Enayatkhani, M. Hasaniazad, S. Faezi et al., "Reverse vaccinology approach to design a novel multi-epitope vaccine candidate against COVID-19: an in silico study," *Journal of Biomolecular Structure and Dynamics*, vol. 39, no. 8, pp. 2857–2872, 2021.

[8] K. O. Kwok, K. K. Li, W. I. Wei et al., "Influenza vaccine uptake, COVID-19 vaccination intention and vaccine hesitancy among nurses: a survey," *International Journal of Nursing Studies*, vol. 114, Article ID 103854, 2021.

[9] K. Bagherzadeh, K. Daneshvarnejad, M. Abbasinazari, and H. azizian, "In silico repositioning for dual inhibitor discovery of SARS-CoV-2 (COVID-19) 3C-like protease and papain-like peptidase," *Medicinal Chemistry*, Article ID 2020040084, 2020.

[10] S. A. Siadati, A. Dadras, M. A. Rezvanfar, A. Beheshti, and S. S. Naeimi, "An urgent industrial scheme both for total synthesis, and for pharmaceutical analytical analysis of umifenovir as an anti-viral API for treatment of COVID-19," *Combinatorial Chemistry & High Throughput Screening*, vol. 25, no. 5, pp. 838–846, 2022.

[11] A. Mirzaie, M. Halaji, F. S. Dehkordi, R. Ranjbar, and H. Noorbazargan, "A narrative literature review on traditional medicine options for treatment of corona virus disease 2019 (COVID-19)," *Complementary Therapies in Clinical Practice*, vol. 40, Article ID 101214, 2020.

[12] S. A. Siadati, M. A. Rezvanfar, E. Babanezhad, A. Beheshti, and M. Payab, "Harmony of operations of some vitamins in controlling the 2019-nCoV virus based on scientific reports," *Chemical Review and Letters*, vol. 3, no. 4, pp. 202–206, 2020.

[13] J. Ghanaat, M. A. Khalilzadeh, and D. Zareyee, "Molecular docking studies, biological evaluation and synthesis of novel 3-mercapto-1, 2, 4-triazole derivatives," *Molecular Diversity*, vol. 25, no. 1, pp. 223–232, 2021.

[14] S. Roy, A. Yadaw, S. Roy et al., "Facile and scalable methodology for the pyrrolo [2, 1-f][1, 2, 4] triazine of remdesivir," *Organic Process Research & Development*, vol. 26, 2021.

[15] B. Mohtat, S. A. Siadati, M. A. Khalilzadeh, and D. Zareyee, "The concern of emergence of multi-station reaction pathways that might make stepwise the mechanism of the 1, 3-dipolar cycloadditions of azides and alkynes," *Journal of Molecular Structure*, vol. 1155, pp. 58–64, 2018.

[16] Z. Hossaini, F. Rostami-Charati, M. Ghambarian, and S. A. Siadati, "Synthesis of a new class of phosphonate derivatives using a three-component reaction of trialkyl phosphites or triaryl phosphites in water," *Phosphorus, Sulfur, and Silicon and the Related Elements*, vol. 190, no. 7, pp. 1177–1182, 2015.

[17] M. Guidi, S. Moon, L. Anghileri, D. Cambié, P. H. Seeberger, and K. Gilmore, "Combining radial and continuous flow synthesis to optimize and scale-up the production of medicines," *Reaction Chemistry & Engineering*, vol. 6, no. 2, pp. 220–224, 2021.

[18] L. Walz, A. J. Cohen, A. P. Rebaza et al., "JAK-inhibitor and type I interferon ability to produce favorable clinical outcomes in COVID-19 patients: a systematic review and meta-analysis," *BMC Infectious Diseases*, vol. 21, no. 1, pp. 47–10, 2021.

[19] P. O. Guimarães, D. Quirk, R. H. Furtado et al., "Tofacitinib in patients hospitalized with covid-19 pneumonia," *New England Journal of Medicine*, vol. 385, no. 5, pp. 406–415, 2021.

[20] A. Maricán, M. J. Simirgiotis, and L. S. Santos, "Asymmetric total synthesis of Tofacitinib," *Tetrahedron Letters*, vol. 54, no. 37, pp. 5096–5098, 2013.

[21] S. G. Ruggeri, J. M. Hawkins, T. M. Makowski, and J. L. Rutherford, "FJ - urban dictionary," U.S. Patent 8, 2012.
[22] S. Zhi, D. Liu, Y. Liu, B. Liu, D. Wang, and L. Chen, "An efficient method for synthesis of tofacitinib citrate," *Journal of Heterocyclic Chemistry*, vol. 53, no. 4, pp. 1259–1263, 2016.
[23] J. Bonanomi, S. Defiore, and B. Novo, US patent 9, 2017.
[24] Y. S. Patil, N. L. Bonde, A. S. Kekan, D. G. Sathe, and A. Das, "An improved and efficient process for the preparation of tofacitinib citrate," *Organic Process Research & Development*, vol. 18, no. 12, pp. 1714–1720, 2014.
[25] W. Cai, J. L. Colony, H. Frost et al., "Investigation of practical routes for the kilogram-scale production of cis-3-Methyl-amino-4-methylpiperidines," *Organic Process Research & Development*, vol. 9, no. 1, pp. 51–56, 2005.
[26] S. T. Rajan, S. Eswaraiah, and R. Satyanarayana, US patent122354-A1, 2016.
[27] B. Xu, Y. Wang, and X. Yang, CN patent 106146507 A, 2016.
[28] C. Xiao, J. Xu, W. Cai et al., CN patent 111995627 A, 2020.
[29] M. J. Frisch, "Gaussian 03 rev. E. 01," 2004, https://www.gaussian.com/.
[30] P. Pakravan and S. A. Siadati, "The possibility of using C20 fullerene and graphene as semiconductor segments for detection, and destruction of cyanogen-chloride chemical agent," *Journal of Molecular Graphics and Modelling*, vol. 75, pp. 80–84, 2017, þ.
[31] R. A. Al-Balushi, I. J. Al-Busaidi, H. Al-Sharji et al., "Synthesis, structural, photo-physical properties and DFT studies of some diarylheptanoids," *Journal of Molecular Structure*, vol. 1264, Article ID 133254, 2022.
[32] M. S. H. Faizi, A. Haque, M. Dege, N. Dege, and M. L. Malysheva, "Crystal structure and DFT study of (E)-2, 6-di-tert-butyl-4-{[2-(pyridin-2-yl) hydrazin-1-ylidene) methyl} phenol," *Acta Crystallographica Section E: Crystallographic Communications*, vol. 73, no. 10, pp. 1449–1452, 2017.
[33] A. Haque, R. A. Al Balushi, I. J. Al-Busaidi et al., "Synthesis, optical spectroscopy, structural, and DFT studies on dimeric iodo-bridged Copper (I) complexes," *Journal of Organometallic Chemistry*, vol. 892, pp. 75–82, 2019.
[34] R. A. Al-Balushi, A. Haque, M. Jayapal et al., "Experimental and theoretical investigation for the level of conjugation in carbazole-based precursors and their mono-di-and polynuclear Pt (II) complexes," *Inorganic Chemistry*, vol. 55, no. 13, pp. 6465–6480, 2016.
[35] S. ., V. Vk, V. Dhiman, K. K. Giri, K. Sharma, M. Zainuddin, and R Mullangi, "Development and validation of a RP-HPLC method for the quantitation of tofacitinib in rat plasma and its application to a pharmacokinetic study," *Biomedical Chromatography: Biomedical Chromatography*, vol. 29, no. 9, pp. 1325–1329, 2015.
[36] European Medicines Agency's (Ema), "The committee for medicinal products for human use (CHMP) is the European medicines agency's (EMA) CHMP," Article ID 425279, 2013, https://www.ema.europa.eu/en/committees/committee-medicinal-products-human-use-chmp.
[37] X. Zhao, M. Chen, B. Huang, H. Ji, and M. Yuan, "Comparative molecular field analysis (CoMFA) and comparative molecular similarity indices analysis (CoMSIA) studies on α(1A)-adrenergic receptor antagonists based on pharmacophore molecular alignment," *International Journal of Molecular Sciences*, vol. 12, no. 10, pp. 7022–7037, 2011.
[38] S. Babu, S. K. Nagarajan, S. Sathish, V. S. Negi, H. Sohn, and T. Madhavan, "Identification of potent and selective JAK1 lead compounds through ligand-based drug design approaches," *Frontiers in Pharmacology*, vol. 13, Article ID 837369, 2022.
[39] R. Parthasarathi, V. Subramanian, D. R. Roy, and P. K. Chattaraj, "Electrophilicity index as a possible descriptor of biological activity," *Bioorganic & Medicinal Chemistry*, vol. 12, no. 21, pp. 5533–5543, 2004.
[40] Ch. Sonia, T. G. Devi, and T. Karlo, "DFT study on the structural and chemical properties of Janus kinase inhibitor drug Baricitinib," *Materials Today Proceedings*, vol. 65, pp. 2586–2595, 2022.